

Using Reinforcement Learning to Optimize the Global and Local Crossing Number

Timo Brand^{1[0009-0004-3111-2045]}, Henry Förster^{1[0000-0002-1441-4189]}, Stephen Kobourov^{1[0000-0002-0477-2724]}, Robin Schukraft¹, Markus Wallinger^{1[0000-0002-2191-4413]}, and Johannes Zink^{1[0000-0002-7398-718X]}

Technical University of Munich, Heilbronn, Germany `{firstname.lastname}@tum.de`

Abstract. We present a novel approach to graph drawing based on reinforcement learning for minimizing the global and the local crossing number, that is, the total number of edge crossings and the maximum number of crossings on any edge, respectively. In our framework, an agent learns how to move a vertex based on a given observation vector in order to optimize its position. The agent receives feedback in the form of local reward signals tied to crossing reduction. To generate an initial layout, we use a stress-based graph-drawing algorithm. We compare our method against force- and stress-based (baseline) algorithms as well as three established algorithms for global crossing minimization on a suite of benchmark graphs. The experiments show mixed results: our current algorithm is mainly competitive for the local crossing number. We see a potential for further development of the approach in the future.

Keywords: Reinforcement Learning · Crossing Minimization · Local Crossing Number · Heuristic.

1 Introduction

Reinforcement-learning breakthroughs made some news in popular media: Shortly after the program AlphaGo [36] had beaten the best human player in the notoriously involved game Go in 2016, the more general programs AlphaGoZero [38] and AlphaZero [37] were able to master games like Go, chess, and Shogi by just being taught the rules and the objectives of the game, but no strategies. It would find out established and even new strategies by playing against itself multiple times – a very successful example of reinforcement learning.

In *reinforcement learning* (RL), an agent acts in some environment in the following way. The agent receives a description of its environment (an *observation vector*), based on which it chooses an action from a set of available actions. These actions may change the environment. The change on the environment is measured. Based on this measurement, the agent receives a *reward*, which is a positive number for a “good” change or a negative number for a “bad” change. The agent tries to maximize its reward. To this end, the agent explores its options by trying different actions for different observation vectors. Internally, the agent uses some learning algorithm. This can be a table (a *Q-table*) of expected rewards

where the rows are the observation vectors and the columns are the available actions. As such tables can become huge for complex tasks and get hard to manage, usually neural networks, whose input is the observation vector and whose output is a recommendation for the next action, are used.

RL is applicable to a variety of tasks, in particular, puzzles, card and board games, and even complex computer games [24,34]. We investigate the following question that arises naturally when applying the RL paradigm to graph drawing:

Can we use reinforcement learning to optimize graph drawings with respect to a given graph drawing aesthetics measure?

The task can be seen as a 1-player game with full information. Not all graph drawing aesthetics are easy to measure (e.g., symmetry). For this paper, we have chosen some well-established and easy-to-quantify aesthetic measures: the total number of edge crossings and the maximum number of edge crossings per edge.

Our Contributions. We present an RL framework for graph drawing to optimize local and global crossings by post-processing a given layout; see Sec. 3. We perform a quantitative analysis on two graph data sets (Rome and Barabási-Albert graphs) comparing our two models against other state-of-the-art approaches; see Sec. 4. We identify strengths and weaknesses of the current approach, which can be seen as a guide for future work on RL in graph drawing; see Secs. 5 and 6. All of our code, benchmark data and results are available on github.¹

2 Preliminaries and Related Work

A drawing of a graph assigns each vertex to a point and each edge to an open Jordan curve not passing through any vertex other than its endpoints. In a straight-line drawing, the edges are straight-line segments.

Crossing Number. For a given drawing Γ of a graph G , the *crossing number* $\text{cr}(\Gamma)$ denotes the number of pairwise edge crossings in Γ . The *crossing number* $\text{cr}(G)$ of a graph G is, among every drawing Γ of G , the minimum of $\text{cr}(\Gamma)$. An often studied variation is the *rectilinear crossing number* $\overline{\text{cr}}(G)$, which denotes, for a graph G , the same value restricted to straight-line drawings of G . The *local crossing number* $\text{lcr}(\Gamma)$ of a drawing Γ is the maximum number of edges that cross a single edge in Γ . The *local crossing number* $\text{lcr}(G)$ and the *rectilinear local crossing number* $\overline{\text{lcr}}(G)$ of a graph G are defined similarly. Computing $\text{cr}(G)$ [15] and $\text{lcr}(G)$ [40] are known to be NP-complete whereas $\overline{\text{cr}}(G)$ [7,33] and $\overline{\text{lcr}}(G)$ [32] are even known to be $\exists\mathbb{R}$ -complete. See Schaefer's [31] survey for more information. Several studies evidence that the number of edge crossings is crucial for the readability of a graph drawing [18,27,28,46]. The local crossing number is a natural variation. Moreover, there are many theoretical results on drawings with $\text{lcr}(\Gamma) = k$, called k -*planar* drawings; see [12,21] for surveys. In the rest of the paper, we only consider straight-line drawings and, hence, (versions of) the rectilinear crossing number. For brevity, we drop the word *rectilinear*.

¹ <https://github.com/j-zink-wuerzburg/rl-4-gd-crossing-reduction>

Graph Layout Methods for Crossing Minimization. First, note that algorithms being force-directed (e.g., the one by Fruchterman–Reingold [14]) or stress-based (e.g., the one by Kamada–Kawai [20]) are well known to produce drawings with practically acceptable crossing numbers, even though they do not explicitly penalize crossings. It has even been shown that, in random geometric graphs, the correlation between the expected crossing number and stress is positive [8]. There exist extensions of force-directed algorithms that interfere with crossings [13] and extra forces improving angles formed at crossings and vertices [3,18].

Several heuristics were developed to directly optimize crossing numbers, in part driven by the annual Graph Drawing Contest,² which, in 2017–2020, focused on crossings in graph drawings. The Karlsruhe Institute of Technology (KIT) team used a simulated-annealing heuristic [9], while the University of Tübingen team employed probabilistic hill climbing [6,26]. Both iteratively select a vertex, typically involved in a small crossing angle, and perturb its position for improvements. Simulated annealing gradually reduces the likelihood of large moves and both algorithms differ in vertex selection, candidate sampling, and strategies for escaping local maxima. From the KIT team, Radermacher et al. [29] investigated variations of the ideas of the simulated annealing-based heuristic for crossing minimization. They provide several *local optimization*-based geometric heuristics. The two most promising methods they investigated are called Vertex Movement and Edge Insertion, where the latter has also been proposed before [5]. The Vertex Movement heuristic starts with an initial drawing and iterates over the vertices in a given order, at each step finding the crossing-minimal position of that vertex in the current drawing. It is noteworthy that the authors departed from subsampling positions for the vertex to be moved and instead find the *optimal* new position for the vertex. The Edge Insertion method instead starts with a planar drawing of a maximal planar subgraph. Then, it inserts the remaining edges. In each step, a new edge e is first inserted and then the drawing is modified so that inserting the next edge only adds few crossings to the drawing. In this process, essentially the Vertex Movement heuristic is applied on the endpoints of e and on the endpoints of the edges crossing e . Also researchers from the University of Arizona competed in the GD contests and published their optimization algorithms that combines linear programming and gradient descent [10] to simultaneously optimize stress and the number of crossings. In a later version being called (SGD)² [1], the gradient restricted to a subset of the vertices is computed for a set of objective functions, and the layout is updated by moving vertices in the direction that maximizes the gradient.

In recent years, there has been some interest in using neural networks to compute drawings [16,22,43,45]. Motivated by the fact that previous approaches struggled to optimize non-differentiable objective functions – such as the number of crossings – Wang et al. [44] introduced SmartGD, a Generative Adversarial Network (GAN)-based deep learning framework.

² See <https://mozart.diei.unipg.it/gdcontest/>.

Reinforcement Learning. There are several frameworks designed for playing arbitrary games, e.g., Google Deepmind’s *OpenSpiel* [23] and *MuZero* [34,48], *Ai Ai* [39], *AmzPlayer* [25]. In these frameworks, the rules of the games, the observation vector, the possible actions, and the reward function must be specified. A sensible encoding of the environment into observation vectors, possible actions, and rewards is crucial for sensible outcomes in a reasonable amount of time; e.g., when encoding graphs, a learning algorithm should not base its decisions on the order of the labels of the graph nodes but rather on the graph structure. Hence, encoding a graph with an adjacency matrix may be problematic because a permutation of the rows and columns gives the same graph but a very different encoding. An RL agent will not necessarily treat both equally, even though all information about the input graph are represented.

The intersection between RL and graph drawing has been relatively small so far. To the best of our knowledge, there is only one unpublished preprint: Safarli, Zhou, and Wang [30] use RL to simulate classic graph-drawing algorithms like force-directed layouts and stress majorization. Their approach uses Q-learning [47] where, for every vertex, an agent with its own Q-table is created. At each iteration, the agent gets an observation where the Q-table reflects the potential reward associated with each action under the current observation: staying or moving in one of the eight cardinal and intercardinal directions. The agent either picks the action with the highest potential reward or a random action to facilitate exploration. The reward is positive if the chosen action reduces the energy or stress in the drawing, while it is negative otherwise. After each action, the Q-table of an agent is updated. The resulting drawings reach a similar quality as the drawings generated by the corresponding classic algorithms.

3 Description of the Approach

We apply RL as a post-processing to existing graph-drawing algorithms in order to improve graph layouts with respect to some objective value. We use as objectives the global crossing number and the local crossing number. We refer to the two corresponding algorithms by RL(GC) and RL(LC).

To obtain a graph-size invariant algorithm, we follow the idea of Safarli, Zhou, and Wang [30], who let an agent “sit” on a vertex v and ask for a direction to move v . Unlike them, we use 16 instead of eight directions to move. Also we do not offer the option of staying because we have the impression that this slows down the process of altering the drawing too much. The algorithm could be realized on an integer grid; however, we decided not to restrict to an integer grid and to allow arbitrary floating-point coordinates instead. Different from Safarli et al., we do not use a separate agent at every vertex. We use one agent that takes the viewpoint of any vertex. To this end, we provide the agent with observation data corresponding to that vertex. This design choice has the purpose of treating vertices that are at structurally similar positions in the graph and the drawing similarly. Moreover, training separate agents for each vertex would make us dependent on the graph and would increase the training time tremendously.

octant	I	II	III	IV	V	VI	VII	VIII
neighbors	.1	.2	0	0	.2	.1	0	.4
vertices	.14	.03	0	.11	.08	.2	.27	.17
closest ngb.	.32	.5	0	0	.25	.67	0	.21
closest vtx.	.32	.28	0	.94	.25	.67	.17	.21
crossings	.1	.2	0	0	.1	.3	0	1.0
local cr.	1	2	0	0	1	2	0	4

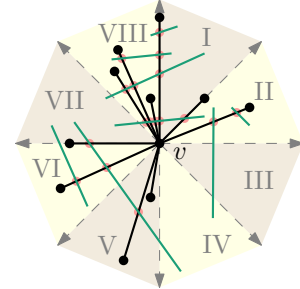


Fig. 1: Local view of a vertex v to its neighborhood in the drawing: v is the center of the eight octants (the rays dividing the octants belong to the clockwise predecessor octant). In each octant, parameters like the number of neighbors and the number of incident crossings are measured. Here, v has degree 10. In the octant VIII, there are four neighbors and ten crossings.

Safarli et al. do not train their agents but rather fill their tables of the agents ad hoc when provided with the input graph. We use a neural network as an agent that is trained on two large data sets. Retrieving knowledge from previous training phases is a core feature of RL.

Observation vector. The vector that the agent gets for a vertex is two-fold: the first part contains information about the local neighborhood in the graph drawing, while the second part contains information about the structural position within the graph (independently of the current position in the graph drawing).

The local neighborhood of a vertex v in the graph drawing is described with respect to the eight octants delimited by the eight octagonal rays going up, up-right, right, down-right, etc. See Fig. 1 for an illustration. The first eight entries count the number of neighboring vertices of v in each octant normalized by the total number of neighbors of v . The second eight entries count the number of vertices in each octant normalized by the total number of vertices. The next eight entries describe the distance to the closest neighbor in the octant, while the next eight entries describe the distance to the closest vertex in the octant. After that, eight entries describe the number of crossings that occur on edges incident to v in the respective octants normalized by the maximum among the eight octants, and eight entries describe the local crossing number of the incident edges of v in the corresponding octants. Finally, two entries describe the current global and local crossing number of the drawing. Together, this yields a vector of length 50 for the local neighborhood. To make the behavior of the agent invariant for rotating and mirroring the coordinate system, whenever we call the agent, we rotate the drawing (i.e., we shift the entries of the octants in the observation vector) such that octant I is the octant with the most crossings and we mirror the drawing such that the octant with the second to most crossings has the minimum number (e.g., in Fig. 1, current octant VIII would be rotated

to octant I, after that, the arrangement would be mirrored to bring the current octant VI to the other side).

To determine the structural positions of the vertices within the graph, we use, once per instance, a graph neural network (a pretrained graph attention network (GAT) [41,42]). This way, we find a 32-dimensional embedding for each vertex. We use principal component analysis (PCA) [19] as a dimension-reduction algorithm on the 32-dimensional embedding to shrink it down to 4 dimensions. We are doing dimension reduction because in our initial experiments this yielded better results than using the 32-dimensional embedding or no global graph information. We add this vector of length 4 to the vector describing the neighborhood in the graph drawing. In total, this gives an observation vector of length 54.

Action Space and Movement of Vertices. In each step, the agent has 16 actions to choose from, which correspond to moving the vertex a direction delimiting two octants or lying in the middle of an octant. Using compass directions these are (22.5 degrees apart): N, NNW, NW, NWW, W, ..., NE, NNE. We remark that the agent only chooses the direction α to move. The move distance is determined as follows. Consider the ray R in direction α emanating from v . If R intersects some edge, take the intersection point p closest to v and move v along R by the distance between v and p times $(1 + \epsilon)$ where ϵ is a random number in $[.01, .1]$. If R does not intersect any edge, we move v by unit distance along R .

Reward Function. The reward function depends on the objective. For the global crossing number, the reward function is the number of removed crossings:

$$\text{reward}_{\text{GC}} = \begin{cases} \overline{\text{cr}}(\Gamma) - \overline{\text{cr}}(\Gamma') & , \text{ if } \overline{\text{cr}}(\Gamma) \neq \overline{\text{cr}}(\Gamma') \\ -0.001 & , \text{ otherwise} \end{cases}$$

Here, Γ is the drawing before and Γ' is the drawing after performing an action. If nothing changes, we give a small negative reward to incentivize alteration.

The reward for the local crossing number combines the change in the local and global crossing number, where m is the total number of edges and $m^*(\Gamma)$ is the number of edges having $\overline{\text{lcr}}(\Gamma)$ crossings on it:

$$\text{reward}_{\text{LC}} = \begin{cases} 10 (\overline{\text{lcr}}(\Gamma) - \overline{\text{lcr}}(\Gamma')) + (\overline{\text{cr}}(\Gamma) - \overline{\text{cr}}(\Gamma')) / m & , \text{ if } \overline{\text{lcr}}(\Gamma) \neq \overline{\text{lcr}}(\Gamma') \\ 0.1(m^*(\Gamma) - m^*(\Gamma)) + (\overline{\text{cr}}(\Gamma) - \overline{\text{cr}}(\Gamma')) / m & , \text{ if } m^*(\Gamma) \neq m^*(\Gamma) \\ & \text{or } \overline{\text{cr}}(\Gamma) \neq \overline{\text{cr}}(\Gamma') \\ -0.001 & , \text{ otherwise} \end{cases}$$

Vertex Selection. We next describe how the agent is assigned to a vertex. Our algorithm is not parallelized, so the agent is only placed at one vertex at a time. When optimizing global crossings, we iteratively assign the agent to a vertex v that is chosen randomly among all vertices with a weighted probability $w_{\text{GC}}(v) = \sum_{e \in \text{inc}(v)} \frac{\overline{\text{cr}}(\Gamma, e)}{\deg(v)}$. Here, Γ is the current drawing, $\overline{\text{cr}}(\Gamma, e)$ is the number of crossings in Γ on edge e , and $\deg(v)$ is the degree of v . The intuition behind this

procedure is that we can move any vertex but moving a vertex that is involved in more crossings is more likely than a vertex involved in fewer crossings. Also, we prefer to move vertices with lower degree because we expect that it is easier for them to eliminate crossings without creating new ones.

Now we consider the setting where we optimize local crossings. Let k be the maximum number of crossings on any edge in the current drawing. We choose a vertex randomly among all vertices that have an incident edge e such that e has k crossings or e intersects an edge having k crossings. To select a vertex v , we use the weighted probability $w_{LC}(v) = \frac{1}{\deg(v)}$. Intuitively vertices with low degree can more easily be moved without too large negative impact elsewhere.

Heuristics. Our algorithm starts with employing a classical graph-drawing algorithm to obtain a baseline drawing. After each step of the RL procedure, we save the currently best drawing. If the agent does not improve upon that drawing within 400 steps, we reset to the previously best drawing.

Agent as Neural Network. Our agent is a neural network that gets as input the observation vector of length 54. The output is a vector of length 16. Each entry of the output vector corresponds to one of the 16 possible actions. In the training phase, the weights of the neural network are adjusted in such a way that actions with positive rewards get higher scores in the output vector and actions with negative rewards get lower scores in the output vector. Each graph of the training data is treated as an episodic environment. We use a proximal policy optimization (PPO) [35] to train the agent, that is, a policy-gradient method typically used in RL. PPO does not explore the way an ϵ -greedy algorithm does. That is, instead of flipping a coin between doing a random and the best decision, a probability distribution over the possible actions is used. Randomness reflects uncertainty and is used for exploration. PPO uses an entropy bonus during training to encourage the policy to resist becoming overconfident too quickly.

4 Experimental Evaluation

We are interested in answering the following research questions:

- RQ1** How well does a reinforcement-learning approach perform in computing drawings with a low global or local crossing number?
- RQ2** How do existing global crossing minimization algorithms perform in finding drawings with low local crossing number?

Implementation details. All code is written in Python 3.12, except for some compute-intensive parts like the crossing computation, which are coded in C++ and included with `pybind11`. The custom environment is implemented on top of the `Gymnasium` library (v1.1.1), and we train a PPO agent using the library `stable-baselines3` (v2.6.0). The GAT, which is used once per graph, is defined in PyTorch Geometric (v2.6.1) and was pre-trained using the `rome` training graphs (see below). During the RL training, we vectorize trainings across 16

parallel environments using `SubProcVecEnv` wrapped in `VecMonitor`. The training is done with an adaptive curriculum, first sampling only `rome` graphs, then mixing them and finally more `BA` graphs (probability of 0.9). In total, we trained the models for 40 million times steps; up to 2,000 per graph. The PPO learning rate is 3×10^{-3} and each batch has a size of 1028. The training was performed with an Intel Xeon Gold 6438Y+ and an Intel Xeon Platinum 8480+ CPU.

Benchmark Graphs. We use two classes of graphs. First, the `rome` graphs³, commonly used in evaluating graph drawing tasks [4,11]. They consist of 11,534 relatively sparse graphs with 10–100 vertices and 9–158 edges. Second, we used `networkx` [17] to generate random graphs; namely, extended Barabási-Albert (`BA`) graphs [2] with 50–150 vertices and preferential attachment parameter $m \in \{1, 2, 3\}$ and reconfiguration parameters $p \in [0, 0.1]$, $q \in [0, 0.2]$. These are larger and tend to have more edges than the `rome` graphs, our dataset has 19–666 edges.

We filter and preprocess both sets. First, we only keep instances that are not planar or disconnected, and then remove all degree-1 vertices from the graph. (After obtaining a drawing with low (local) crossing number, degree-1 vertices can be inserted again in an ϵ -neighborhood of the adjacent vertex without introducing any crossings.) For the extended Barabási-Albert graphs, this filtered out most of the graph with parameter $m = 1$ as these are very often planar. Finally, an initial drawing used as input to the algorithms is obtained with the Kamada–Kawai algorithm [20], which uses spring forces between vertices proportional to their graph-theoretic distance. In initial experiments, it created drawings with usually fewer global and local crossings than the Fruchterman–Reingold algorithm [14]. The 8,252 `rome` graphs remaining after the filtering procedure were split into 6,602 graphs for training our RL model and 1,650 graphs for testing. Similarly, 1,000 `BA` graphs were used for training and 500 for testing.

Benchmark Algorithms. As a generic baseline, we use the algorithms Kamada–Kawai (KK) and Fruchterman–Reingold (FR), both implemented in `networkx`. KK also produces the initial layout used as input to the other algorithms. We also compare with another machine-learning-based model, namely, the *GAN-based framework* SmartGD [44]. In particular, the authors released a model trained to minimize the crossing number, which we use in our evaluation⁴. Like our algorithm, it was trained on the `rome` graphs. Regarding previous heuristic solutions, we compare to (SGD)² [1]⁵, to the *geometric local-optimization* approaches Vertex Movement (VM) and Edge Insertion (EI) [29],⁶ and to the *probabilistic hill-climbing* method Tübingen-Bus (TB). Note that, while TB was originally designed for minimizing the number of crossings in upward drawings, we could easily adjust it to drop the upward constraint [26]⁷. We use the default parameters given in the implementations or papers; see Sec. 2 for details on the algorithms.

³ <http://graphdrawing.org/data.html>

⁴ <https://github.com/yolandalalala/SmartGD>

⁵ <https://github.com/tiga1231/graph-drawing/tree/sgd>

⁶ Source code obtained from the authors

⁷ Source code obtained from the authors

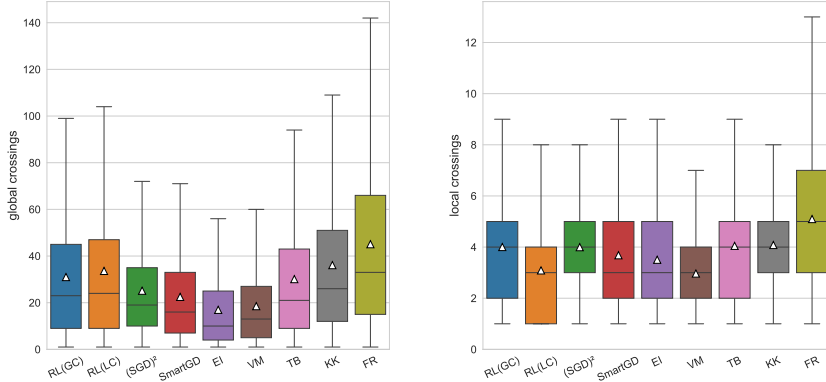


Fig. 2: The global (left) and local (right) crossing number on the `rome` graphs.

Results. We run all algorithms on the testing sets of the benchmark graphs. From the generated layouts, we record the global and local crossing numbers and the running time. We use a time limit of 900 seconds per graph and algorithm. All experiments were run on a server with Intel Xeon Platinum 8480+ CPUs using Python 3.12. C++ sources were compiled with GCC 14.3. While training of the RL models was done in parallel, the evaluations were run on a single CPU with 512GB of memory available without any memory limit being enforced. We remark that SmartGD, $(SGD)^2$ and KK/FR from `networkx` are Python-based, while the other algorithms for comparison are implemented in C++.

For the `rome` graphs, the results on the global and local crossing number are represented in a box plot in Fig. 2. An illustration of the pairwise wins in percent of the test instances is given in Fig. 5 in Sec. B. Recall that in box plots, the full range represents the values for all instances (except outliers), with 50% falling into the colored rectangles. The lines in the middle are the median, and the triangle marks the mean value.

For the global crossing number, we can see that EI and VM computes drawings with the lowest crossing number, and also has the smallest range of crossing numbers. Next is SmartGD and $(SGD)^2$. After that TB follows, followed by RL(GC) and RL(LC), which just slightly improve over KK. This picture changes for the local crossing number, where RL(LC) and VM achieve the lowest values most of the time. They are followed by EI and SmartGD. After that, RL(GC), $(SGD)^2$, TB, and KK perform similarly.

The running times of the algorithms on the `rome` graphs are illustrated in Fig. 3a. We observe that only $(SGD)^2$, EI, and VM have a large running time; the other algorithms solve all instances in less than 6 seconds. Interestingly, we can see that $(SGD)^2$ requires about the same running time for all instances, likely due to performing a fixed number of iterations in the stochastic gradient descent.

For our second set of instances, the extended Barabási-Albert graphs, the results on the global and local crossing computations can be found in the box plots of Fig. 4 and Fig. 7 in Sec. B. Fig. 4 includes all instances but excludes

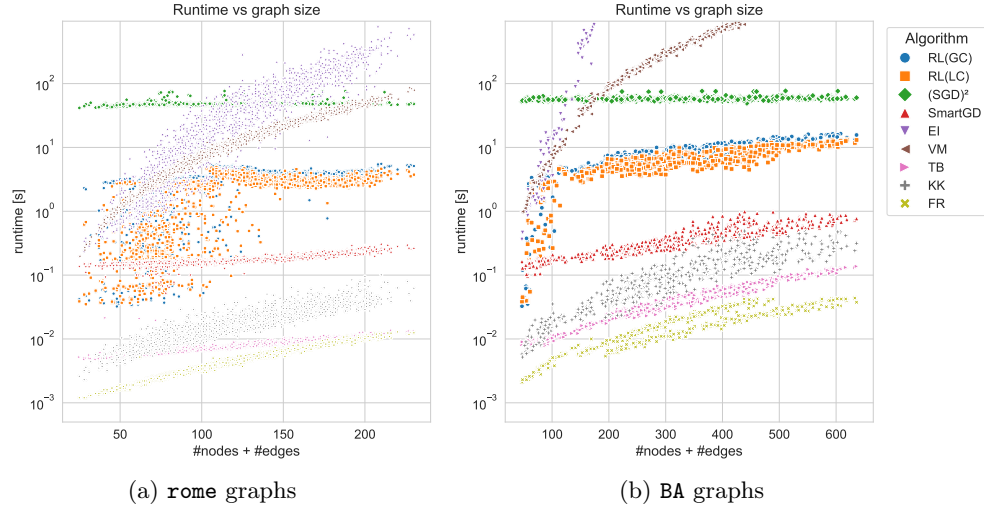


Fig. 3: Scatter plots of the runtimes vs. graph sizes. A mark represents a graph.

the algorithms **EI** and **VM**, which solved only 91 and 377 instances in time, respectively. In contrast, Fig. 7 includes all algorithms but considers only the 91 graphs where every algorithm returned a drawing. The pairwise win percentage of algorithms compared to each other is given in Fig. 6 in Sec. B.

When included, **EI** achieves the best values for the global crossing number and **VM** the best values for the local crossing number with the other one ranking second (**EI** almost on par with **RL(LC)** for the local crossing number). Otherwise, for the global crossing number, **(SGD)²** ranks before **TB**, which ranks before all others with **SmartGD** and **FR** performing worst. For the local crossing number, the difference between the algorithms is small. **(SGD)²** and **RL(LC)** perform best, followed by the three algorithms **RL(GC)**, **TB**, and **KK**. **SmartGD** ranks last.

The running times are visualized in Fig. 3b. We see a similar trend as on the **rome** graphs. Note that **EI** and **VM** appear very high in the plots due to their timeouts after 900 seconds. The median running time of **(SGD)²** roughly doubles compared to the **rome** graphs but stays similar across various **BA** graph sizes.

In pairwise comparison, most performance differences between the algorithms display statistical significance when computing the Wilcoxon Holm-adjusted *p*-values; Sec. A. Also, we show sample output drawings of all algorithms; Sec. C.

5 Discussion

RQ1. We first analyze the competitiveness in terms of running time. Here, we find a natural hierarchy of algorithms that applies to both **rome** and **BA**: (i) **KK**, **TB**, and **FR** are the fastest heuristic solutions with median running times between 0.01s and 0.1s, significantly outperforming all other heuristics on the **rome** graphs and displaying advantages over the rest on the **BA** graphs.

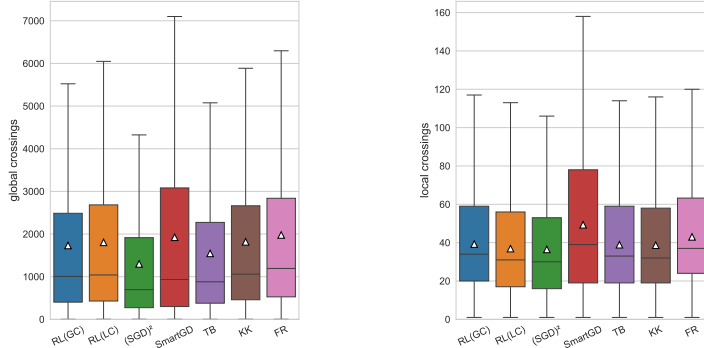


Fig. 4: The global (left) and local (right) crossing number on the BA graphs on all instances, excluding the algorithms EI and VM, which did not finish all instances.

(ii) SmartGD has the next fastest running times, which range between 0.1s and 1s on all graphs. (iii) RL(GC) and RL(LC) have mean running times in the range 1–10s on all graphs. (iv) $(SGD)^2$ displays the most consistent running time with a median of 47.8s for rome graphs and 58.4s for BA graphs. (v) While EI and VM have a slightly lower running times than $(SGD)^2$ for most of the rome graphs, they encounter serious running time issues on the 500 BA graphs. EI only managed to find solutions for 91 graphs whereas VM managed 377 graphs within a 900s time limit per instance. There is a strong correlation with the graph size recognizable. So, in terms of running time, our RL approach displays competitive behavior with respect to established approaches.

When it comes to the global and local crossing numbers in the produced drawings, our approaches behave quite different compared to the other algorithms. For the global crossing number, our RL methods perform quite poorly, while, for the local crossing number, our RL methods are among the best-performing approaches. For the comparison of the global crossing number, we consider only RL(GC), and, for the local crossing number, we consider only RL(LC).

In comparison to the slower heuristics $(SGD)^2$, EI and VM, we observe that our heuristics RL(GC) shows noticeably worse mean global crossing numbers. This observation is also strengthened by considering the pairwise win percentages.

The picture is different for the local crossing number. On the rome graphs, RL(LC) wins (loses) against $(SGD)^2$, SmartGD, EI, VM, and TB in 64.1% (13.2%), 54.1% (15.6%) 44.5% (19.8%), 27.9% (27.7%), and 66.6% (8.9%) of test cases, respectively. So RL(LC) outperforms $(SGD)^2$, SmartGD, EI, and TB while it is pretty much on par with VM, but up to one order of magnitude faster. On the BA graphs, RL(LC) wins (loses) against $(SGD)^2$, SmartGD, EI, VM, and TB in 45.0% (46.0%), 84.4% (9.4%) 85.8% (5.8%), 32.4% (57.0%), and 63.2% (25.4%) of test cases, respectively (in case of a time out, it is a win for the algorithm finishing). So, RL(LC) outperforms SmartGD, EI, and TB, is on par with $(SGD)^2$, and a bit behind VM. Note, however, that RL(LC) is almost one order of magnitude faster than $(SGD)^2$ and VM did not even finish 123 out of 500 instances in time.

We conclude that our RL approach is a preferable choice for optimizing the local crossing, but not an option of choice for the global crossing number. This recommendation should be taken with a grain of salt since our RL procedure is a post-processing (here for KK) and the competitor algorithms do not explicitly optimize the local crossing number. But, to the best of our knowledge, there is no general algorithm explicitly optimizing the local crossing number yet.

RQ2. Comparing the performance of the existing heuristics ignoring our RL methods, our experiments indicate a strong correlation between performance with respect to global crossing number and performance with respect to local crossing number. In fact, the hierarchy of performance appears to remain the same with one exception. The heuristic EI beats VM in terms of global crossing number but then performs worse in terms of local crossing number.

Our results indicate that there is a strong correlation between global and local crossing number but an algorithm optimized for the local crossing number should beat an approach optimized for global crossing number as indicated by RL(LC).

Limitations. We trained our models only on two graph classes and cannot infer from the results that our approach generalizes to arbitrary graphs. While the running times of our approaches are better than the ones for EI and VM, we still see slower running times than for some existing algorithms resulting in limited scalability for larger graphs. We believe that this might be remedied by a more efficient implementation, e.g., completely in C++. Finally, in our experiments we restricted ourselves to a single initial layouting method and it remains unclear how strongly the performance depends on the initial layout.

6 Conclusion and Future Work

We have presented a novel post-processing procedure to optimize the global and the local crossing number. We are among the first to optimize the local crossing number, for which we achieve good results in the comparisons. Still, the results are far from perfect as the comparisons with the global crossing number indicates. Our hope was to identify some general AI-framework into which we simply plug in our problem. At least to us, it turned out to be more involved than just using an out-of-the-box solution since the performance and (quick) learning success heavily depends upon the modeling of the problem, the observation vector, the available actions, etc. A different overall modeling might perform better.

Future Work. For better performance, one could increase the amount and diversity of training data by including a wider range of benchmark graphs and much longer training times. It would be good to have a graph set with known local crossing numbers. A different design of the vertex selection, observation vector, and action space might also lead to better results. More generally, we plan to investigate different RL approaches and frameworks. We believe that the general idea is applicable to arbitrary quantifiable objectives, which may be tested.

References

1. Ahmed, R., De Luca, F., Devkota, S., Kobourov, S., Li, M.: Multicriteria scalable graph drawing via stochastic gradient descent, (sgd)². *IEEE Transactions on Visualization and Computer Graphics* **28**(6), 2388–2399 (2022). <https://doi.org/10.1109/TVCG.2022.3155564>
2. Albert, R., Barabási, A.L.: Topology of evolving networks: local events and universality. *Physical review letters* **85**(24), 5234 (2000)
3. Argyriou, E.N., Bekos, M.A., Symvonis, A.: Maximizing the total resolution of graphs. *Comput. J.* **56**(7), 887–900 (2013). <https://doi.org/10.1093/COMJNL/BXS088>, <https://doi.org/10.1093/comjnl/bxs088>
4. Bartolomeo, S.D., Crnovrsanin, T., Saffo, D., Puerta, E., Wilson, C., Dunne, C.: Evaluating graph layout algorithms: A systematic review of methods and best practices. *Comput. Graph. Forum* **43**(6) (2024). <https://doi.org/10.1111/CGF.15073>
5. Batini, C., Talamo, M., Tamassia, R.: Computer aided layout of entity relationship diagrams. *J. Syst. Softw.* **4**(2–3), 163–173 (1984). [https://doi.org/10.1016/0164-1212\(84\)90006-2](https://doi.org/10.1016/0164-1212(84)90006-2)
6. Bekos, M.A., Förster, H., Geckeler, C., Holländer, L., Kaufmann, M., Spallek, A.M., Splett, J.: A heuristic approach towards drawings of graphs with high crossing resolution. *Comput. J.* **64**(1), 7–26 (2021). [https://doi.org/10.1093/comjnl/bxz133](https://doi.org/10.1093/COMJNL/BXZ133)
7. Bienstock, D.: Some provably hard crossing number problems. *Discrete & Computational Geometry* **6**, 443–459 (1991)
8. Chimani, M., Döring, H., Reitzner, M.: Crossing numbers and stress of random graphs. In: Biedl, T., Kerren, A. (eds.) *Proc. 26th International Symposium on Graph Drawing and Network Visualization (GD 2018)*. Lecture Notes in Computer Science, vol. 11282, pp. 255–268. Springer (2018). https://doi.org/10.1007/978-3-030-04414-5_18
9. Demel, A., Dürrschnabel, D., Mchedlidze, T., Radermacher, M., Wulf, L.: A greedy heuristic for crossing-angle maximization. In: Biedl, T., Kerren, A. (eds.) *Graph Drawing and Network Visualization - 26th International Symposium, GD 2018, Barcelona, Spain, September 26–28, 2018, Proceedings*. Lecture Notes in Computer Science, vol. 11282, pp. 286–299. Springer (2018). https://doi.org/10.1007/978-3-030-04414-5_20, https://doi.org/10.1007/978-3-030-04414-5_20
10. Devkota, S., Ahmed, A.R., Luca, F.D., Isaacs, K.E., Kobourov, S.G.: Stress-plus-x (SPX) graph layout. In: Archambault, D., Tóth, C.D. (eds.) *Graph Drawing and Network Visualization - 27th International Symposium, GD 2019, Prague, Czech Republic, September 17–20, 2019, Proceedings*. Lecture Notes in Computer Science, vol. 11904, pp. 291–304. Springer (2019). https://doi.org/10.1007/978-3-03-35802-0_23, https://doi.org/10.1007/978-3-03-35802-0_23
11. Di Battista, G., Garg, A., Liotta, G., Tamassia, R., Tassinari, E., Vargiu, F.: An experimental comparison of four graph drawing algorithms. *Computational Geometry* **7**(5–6), 303–325 (1997)
12. Didimo, W., Liotta, G., Montecchiani, F.: A survey on graph drawing beyond planarity. *ACM Comput. Surv.* **52**(1), 4:1–4:37 (2019). <https://doi.org/10.1145/3301281>, <https://doi.org/10.1145/3301281>
13. Didimo, W., Liotta, G., Romeo, S.A.: Topology-driven force-directed algorithms. In: Brandes, U., Cornelsen, S. (eds.) *Graph Drawing - 18th International Symposium, GD 2010, Konstanz, Germany, September 21–24, 2010. Revised Selected Papers*. Lecture Notes in Computer Science, vol. 6502, pp. 165–176. Springer

- (2010). https://doi.org/10.1007/978-3-642-18469-7_15, https://doi.org/10.1007/978-3-642-18469-7_15
14. Fruchterman, T.M., Reingold, E.M.: Graph drawing by force-directed placement. Software: Practice and experience **21**(11), 1129–1164 (1991)
 15. Garey, M.R., Johnson, D.S.: Crossing number is np-complete. SIAM Journal on Algebraic Discrete Methods **4**(3), 312–316 (1983). <https://doi.org/10.1137/0604033>, <https://doi.org/10.1137/0604033>
 16. Giovannangeli, L., Lalanne, F., Auber, D., Giot, R., Bourqui, R.: Deep neural network for drawing networks, (*DNN*)². In: Purchase, H.C., Rutter, I. (eds.) Graph Drawing and Network Visualization - 29th International Symposium, GD 2021, Tübingen, Germany, September 14-17, 2021, Revised Selected Papers. Lecture Notes in Computer Science, vol. 12868, pp. 375–390. Springer (2021). https://doi.org/10.1007/978-3-030-92931-2_27, https://doi.org/10.1007/978-3-030-92931-2_27
 17. Hagberg, A., Swart, P.J., Schult, D.A.: Exploring network structure, dynamics, and function using networkx. Tech. rep., Los Alamos National Laboratory (LANL), Los Alamos, NM (United States) (2008), function used to generate extended Barabási-Albert graphs: https://networkx.org/documentation/stable/reference/generated/networkx.generators.random_graphs.extended_barabasi_albert_graph.html
 18. Huang, W., Eades, P., Hong, S., Lin, C.: Improving multiple aesthetics produces better graph drawings. J. Vis. Lang. Comput. **24**(4), 262–272 (2013). <https://doi.org/10.1016/JJVLC.2011.12.002>, <https://doi.org/10.1016/j.jvlc.2011.12.002>
 19. Jolliffe, I.T.: Principal Component Analysis. Springer Series in Statistics, Springer, 2nd edn. (2002). <https://doi.org/10.1007/b98835>
 20. Kamada, T., Kawai, S.: An algorithm for drawing general undirected graphs. Information Processing Letters **31**(1), 7–15 (1989). [https://doi.org/10.1016/0020-0190\(89\)90102-6](https://doi.org/10.1016/0020-0190(89)90102-6)
 21. Kobourov, S.G., Liotta, G., Montecchiani, F.: An annotated bibliography on 1-planarity. Comput. Sci. Rev. **25**, 49–67 (2017). <https://doi.org/10.1016/JCOSREV.2017.06.002>, <https://doi.org/10.1016/j.cosrev.2017.06.002>
 22. Kwon, O., Ma, K.: A deep generative model for graph layout. IEEE Trans. Vis. Comput. Graph. **26**(1), 665–675 (2020). <https://doi.org/10.1109/TVCG.2019.2934396>
 23. Lanctot, M., Lockhart, E., Lespiau, J.B., Zambaldi, V., Upadhyay, S., Pérolat, J., Srinivasan, S., Timbers, F., Tuyls, K., Omidshafiei, S., Hennes, D., Morrill, D., Muller, P., Ewalds, T., Faulkner, R., Kramár, J., Vylder, B.D., Saeta, B., Bradbury, J., Ding, D., Borgeaud, S., Lai, M., Schrittweiser, J., Anthony, T., Hughes, E., Danihelka, I., Ryan-Davis, J.: OpenSpiel: A framework for reinforcement learning in games. CoRR **abs/1908.09453** (2019)
 24. Mnih, V., Kavukcuoglu, K., Silver, D., Rusu, A.A., Veness, J., Bellemare, M.G., Graves, A., Riedmiller, M.A., Fidjeland, A., Ostrovski, G., Petersen, S., Beattie, C., Sadik, A., Antonoglou, I., King, H., Kumaran, D., Wierstra, D., Legg, S., Hassabis, D.: Human-level control through deep reinforcement learning. Nature **518**(7540), 529–533 (2015). <https://doi.org/10.1038/NATURE14236>
 25. P., D.: AmzPlayer: A modern player for Zillions. <http://www.polyomino.com/amzplayer/> (2023)
 26. Pfister, M.: Personal communication (2025)
 27. Purchase, H.C.: Effective information visualisation: a study of graph drawing aesthetics and algorithms. Interacting with Computers **13**(2), 147–162 (2000). [https://doi.org/10.1016/S0953-5438\(00\)00032-1](https://doi.org/10.1016/S0953-5438(00)00032-1)

28. Purchase, H.C., Carrington, D.A., Allder, J.: Empirical evaluation of aesthetics-based graph layout. *Empirical Software Engineering* **7**(3), 233–255 (2002). <https://doi.org/10.1023/A:1016344215610>
29. Radermacher, M., Reichard, K., Rutter, I., Wagner, D.: Geometric heuristics for rectilinear crossing minimization. *Journal of Experimental Algorithmics (JEA)* **24**, 1–21 (2019)
30. Safarli, I., Zhou, Y., Wang, B.: Interpreting graph drawing with multi-agent reinforcement learning. *CoRR* **abs/2011.00748** (2020)
31. Schaefer, M.: The graph crossing number and its variants: A survey. *The Electronic Journal of Combinatorics* (2013 (last updated in 2024))
32. Schaefer, M.: Complexity of geometric k-planarity for fixed k. *J. Graph Algorithms Appl.* **25**(1), 29–41 (2021). <https://doi.org/10.7155/JGAA.00548>, <https://doi.org/10.7155/jgaa.00548>
33. Schaefer, M.: On the complexity of some geometric problems with fixed parameters. *J. Graph Algorithms Appl.* **25**(1), 195–218 (2021). <https://doi.org/10.7155/JGAA.00557>, <https://doi.org/10.7155/jgaa.00557>
34. Schrittwieser, J., Antonoglou, I., Hubert, T., Simonyan, K., Sifre, L., Schmitt, S., Guez, A., Lockhart, E., Hassabis, D., Graepel, T., Lillicrap, T.P., Silver, D.: Mastering atari, go, chess and shogi by planning with a learned model. *Nature* **588**(7839), 604–609 (2020). <https://doi.org/10.1038/S41586-020-03051-4>, <https://doi.org/10.1038/s41586-020-03051-4>
35. Schulman, J., Wolski, F., Dhariwal, P., Radford, A., Klimov, O.: Proximal policy optimization algorithms. *CoRR* **abs/1707.06347** (2017)
36. Silver, D., Huang, A., Maddison, C.J., Guez, A., Sifre, L., van den Driessche, G., Schrittwieser, J., Antonoglou, I., Panneershelvam, V., Lanctot, M., Dieleman, S., Grewe, D., Nham, J., Kalchbrenner, N., Sutskever, I., Lillicrap, T.P., Leach, M., Kavukcuoglu, K., Graepel, T., Hassabis, D.: Mastering the game of Go with deep neural networks and tree search. *Nature* **529**(7587), 484–489 (2016). <https://doi.org/10.1038/NATURE16961>
37. Silver, D., Hubert, T., Schrittwieser, J., Antonoglou, I., Lai, M., Guez, A., Lanctot, M., Sifre, L., Kumaran, D., Graepel, T., Lillicrap, T., Simonyan, K., Hassabis, D.: A general reinforcement learning algorithm that masters chess, shogi, and Go through self-play. *Science* **362**(6419), 1140–1144 (2018). <https://doi.org/10.1126/science.aar6404>
38. Silver, D., Schrittwieser, J., Simonyan, K., Antonoglou, I., Huang, A., Guez, A., Hubert, T., Baker, L., Lai, M., Bolton, A., Chen, Y., Lillicrap, T.P., Hui, F., Sifre, L., van den Driessche, G., Graepel, T., Hassabis, D.: Mastering the game of Go without human knowledge. *Nature* **550**(7676), 354–359 (2017). <https://doi.org/10.1038/NATURE24270>
39. Tavener, S.: Ai Ai: a Java-based general game playing engine. <http://mrraow.com/index.php/aiai-home/> (2025)
40. Urschel, J.C., Wellens, J.: Testing gap k -planarity is np-complete. *Inf. Process. Lett.* **169**, 106083 (2021). <https://doi.org/10.1016/J.IPL.2020.106083>, <https://doi.org/10.1016/j.ipl.2020.106083>
41. Velickovic, P., Cucurull, G., Casanova, A., Romero, A., Liò, P., Bengio, Y.: Graph attention networks. *CoRR* **abs/1710.10903** (2017)
42. Velickovic, P., Fedus, W., Hamilton, W.L., Liò, P., Bengio, Y., Hjelm, R.D.: Deep graph infomax. *CoRR* **abs/1809.10341** (2018)
43. Wang, X., Yen, K., Hu, Y., Shen, H.: DeepGD: A deep learning framework for graph drawing using GNN. *IEEE Computer Graphics and Applications* **41**(5), 32–

- 44 (2021). <https://doi.org/10.1109/MCG.2021.3093908>, <https://doi.org/10.1109/MCG.2021.3093908>
44. Wang, X., Yen, K., Hu, Y., Shen, H.W.: SmartGD: A gan-based graph drawing framework for diverse aesthetic goals. *IEEE Transactions on Visualization and Computer Graphics* **30**(8), 5666–5678 (2023)
45. Wang, Y., Jin, Z., Wang, Q., Cui, W., Ma, T., Qu, H.: Deepdrawing: A deep learning approach to graph drawing. *IEEE Trans. Vis. Comput. Graph.* **26**(1), 676–686 (2020). <https://doi.org/10.1109/TVCG.2019.2934798>, <https://doi.org/10.1109/TVCG.2019.2934798>
46. Ware, C., Purchase, H.C., Colpoys, L., McGill, M.: Cognitive measurements of graph aesthetics. *Information Visualization* **1**(2), 103–110 (2002). <https://doi.org/10.1057/palgrave.ivs.9500013>
47. Watkins, C.J.C.H., Dayan, P.: Technical note q-learning. *Mach. Learn.* **8**, 279–292 (1992). <https://doi.org/10.1007/BF00992698>, <https://doi.org/10.1007/BF00992698>
48. Werner Duvaud, A.H.: Muzero general: Open reimplementation of muzero. <https://github.com/werner-duvaud/muzero-general> (2019)

A Statistical Significance

Table 1: Wilcoxon–Holm-adjusted p -values for the global crossing number computed by the algorithms. Above the diagonal are the p -values for the `rome` graphs, below the diagonal for the BA graphs. The BA graphs are restricted to the 91 instances solved by all algorithms.

	RL(GC)	RL(LC)	(SGD) ²	SmartGD	EI	VM	TB	KK	FR
RL(GC)	–	0.000	0.000	0.000 0.000 0.000 0.000 0.000 0.000					
RL(LC)	0.000	–	0.000	0.000 0.000 0.000 0.000 0.000 0.000					
(SGD) ²	0.016	0.000	–	0.000 0.000 0.000 0.000 0.000 0.000					
SmartGD	0.000	0.000	0.236	– 0.000 0.000 0.000 0.000 0.000 0.000					
EI	0.000	0.000	0.000	0.000	– 0.000 0.000 0.000 0.000 0.000 0.000				
VM	0.000	0.000	0.000	0.000 0.000	– 0.000 0.000 0.000 0.000 0.000 0.000				
TB	0.236	0.000	0.002	0.000 0.000 0.000	0.000 0.000 0.000	– 0.000 0.000 0.000			
KK	0.000	0.000	0.000	0.000 0.000 0.000 0.000	0.000 0.000 0.000 0.000	– 0.000 0.000 0.000			
FR	0.000	0.000	0.000	0.000 0.000 0.000 0.000 0.000	0.000 0.000 0.000 0.000 0.000	–			

Table 2: Wilcoxon–Holm-adjusted p -values for the local crossing number computed by the algorithms. Above the diagonal are the p -values for the `rome` graphs, below the diagonal for the BA graphs. The BA graphs are restricted to the 91 instances solved by all algorithms.

	RL(GC)	RL(LC)	(SGD) ²	SmartGD	EI	VM	TB	KK	FR
RL(GC)	–	0.000	0.956	0.000 0.000 0.000 0.537 0.011 0.000					
RL(LC)	0.000	–	0.000	0.000 0.000 0.004 0.000 0.000 0.000					
(SGD) ²	1.000	0.001	–	0.000 0.000 0.000 0.537 0.092 0.000					
SmartGD	1.000	0.000	1.000	– 0.000 0.000 0.000 0.000 0.000 0.000					
EI	0.000	0.498	0.000	0.000	– 0.000 0.000 0.000 0.000 0.000 0.000				
VM	0.000	0.001	0.000	0.000 0.200	0.000 0.000 0.000	– 0.000 0.000 0.000			
TB	1.000	0.000	1.000	1.000 0.000 0.000	0.000 0.000 0.000	– 0.537 0.000			
KK	1.000	0.000	0.662	0.433 0.000 0.000	1.000	0.000 0.000 0.000	– 0.000 0.000 0.000		
FR	0.000	0.000	0.000	0.000 0.000 0.000 0.000 0.000	0.000 0.000 0.000 0.000 0.000	–			

B Additional Statistical Figures

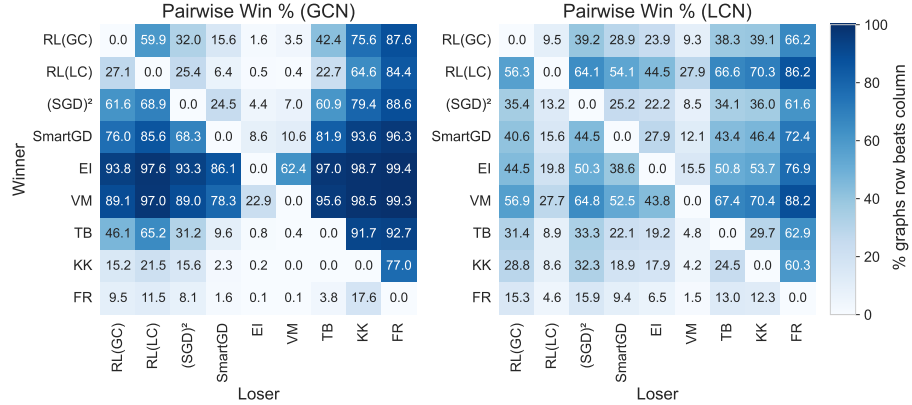


Fig. 5: Pairwise win percentage on the `rome` graphs.

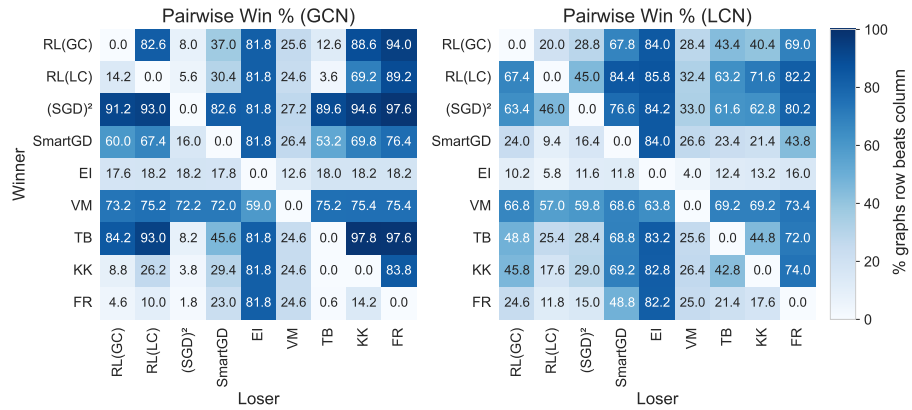


Fig. 6: Pairwise win percentage on the `BA` graphs. If an algorithm did not finish a graph in time, while the other algorithm does, this is counted as a loss for the algorithm that did not finish.

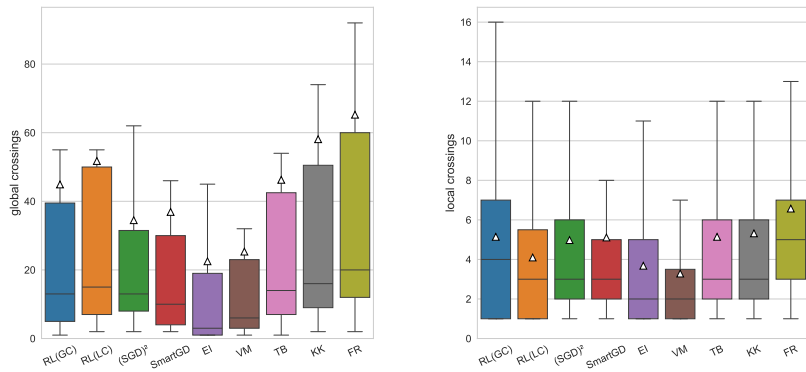


Fig. 7: The global (left) and local (right) crossing number on the BA graphs only on those instances where all algorithms produced a drawing.

C Sample Outputs of All Algorithms

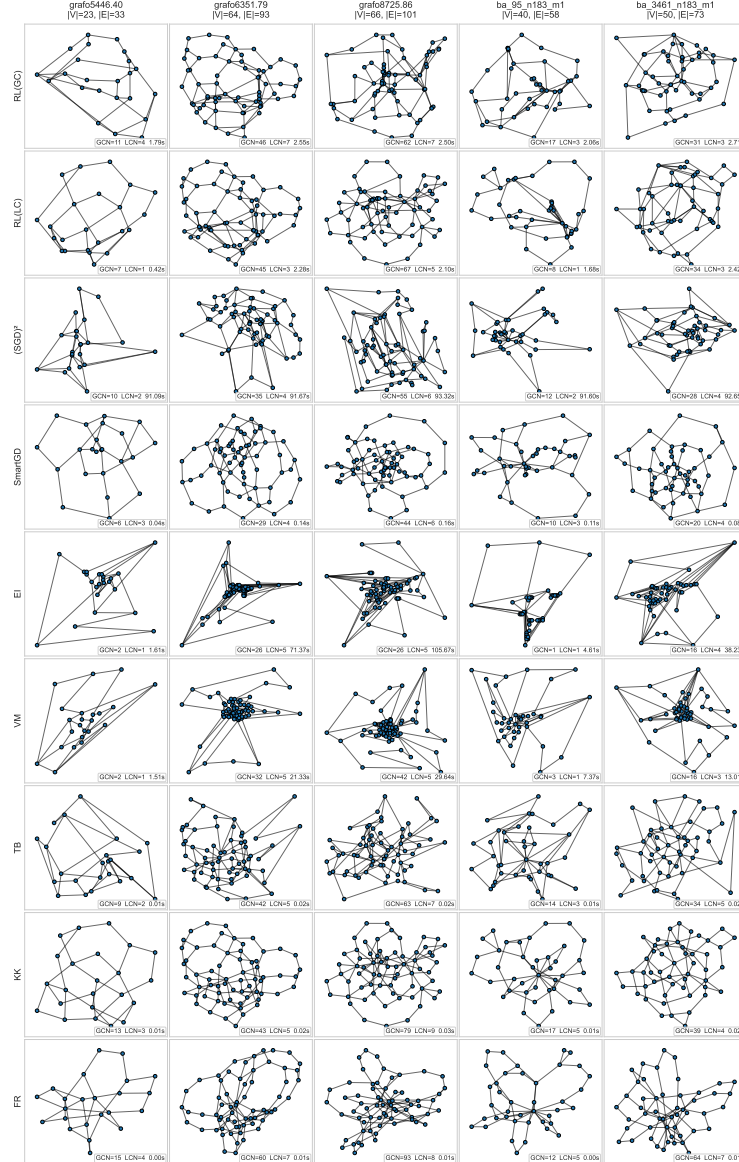


Fig. 8: Example drawings obtained from the different algorithms on 5 randomly selected rome and BA graphs, respectively. Included are the global crossing number (GCN) and local crossing number (LCN) of the drawings as well as the running time.